Tree Physiology 42, 337–350
https://doi.org/10.1093/treephys/tpab100

Research paper

Parenchyma underlies the interspecific variation of xylem hydraulics and carbon storage across 15 woody species on a subtropical island in Japan

Kiyosada Kawai[1,2,5], Kanji Minagi[1], Tomomi Nakamura[1], Shin-Taro Saiki[3], Kenichi Yazaki[3,4] and Atsushi Ishida[1]

[1]Center for Ecological Research, Kyoto University, Hirano 2 509-3 Otsu, Shiga 520-2113, Japan; [2]Forestry Division, Japan International Research Center for Agricultural Sciences, Ohwashi 1-1 Tsukuba, Ibaraki 305-8686, Japan; [3]Department of Plant Ecology, Forestry and Forest Products Research Institute, Matsunosato 1, Tsukuba, Ibaraki 305-8687, Japan; [4]Soil-Plant Ecosystem Group, Hokkaido Research Center, Forestry and Forest Products Research Institute, Hitsujigaoka 7, Sapporo, Hokkaido 062-8516, Japan; [5]Corresponding author (kawaik@affrc.go.jp)

Received October 17, 2020; accepted July 7, 2021; handling Editor Jordi Martinez-Vilalta

Parenchyma is an important component of the secondary xylem. It has multiple functions and its fraction is known to vary substantially across angiosperm species. However, the physiological significance of this variation is not yet fully understood. Here, we examined how different types of parenchyma (ray parenchyma [RP], axial parenchyma [AP] and AP in direct contact with vessels [APV]) are coordinated with three essential xylem functions: water conduction, storage of non-structural carbohydrate (NSC) and mechanical support. Using branch sapwood of 15 co-occurring drought-adapted woody species from the subtropical Bonin Islands, Japan, we quantified 10 xylem anatomical traits and examined their linkages to hydraulic properties, storage of soluble sugars and starch and sapwood density. The fractions of APV and AP in the xylem transverse sections were positively correlated with the percentage loss of conductivity in the native condition, whereas that of RP was negatively correlated with the maximum conductivity across species. Axial and ray parenchyma fractions were positively associated with concentrations of starch and NSC. The fraction of parenchyma was independent of sapwood density, regardless of parenchyma type. We also identified a negative relationship between hydraulic conductivity and NSC storage and sapwood density, mirroring the negative relationship between the fractions of parenchyma and vessels. These results suggest that parenchyma fraction underlies species variation in xylem hydraulic and carbon use strategies, wherein xylem with a high fraction of AP may adopt an embolism repair strategy through an increased starch storage with low cavitation resistance.

Keywords: axial parenchyma, drought-induced embolism, functional xylem anatomy, oceanic island, ray parenchyma, subtropical forest.

Introduction

The secondary xylem in angiosperms generally consists of three distinct cell types: vessels, fibers and parenchyma, which have properties associated with different functions. Vessels conduct water from the soil to the photosynthetic leaves, fibers provide mechanical strength to support the plant body and living parenchyma stores and transports water, non-structural carbohydrate (NSC) and nutrients, as well as providing defense against pathogens (Tyree and Zimmermann 2002, Pratt and Jacobsen 2017, Morris et al. 2016*a*, 2020). The form, arrangement and fraction of these cell types vary considerably among species, and their functional significance has been investigated, particularly for vessels and fibers (Hacke and Sperry 2001, Pratt and Jacobsen 2017, Carlquist 2018). For example, vessels of a greater diameter are associated with the greater xylem hydraulic conductivity and lower resistance, especially in the

process of freeze–thaw-induced embolism among woody plant species (Davis et al. 1999, Tyree and Zimmermann 2002). A higher fiber wall fraction and lower fiber lumen fraction lead to a higher wood density and greater modulus of rupture (Jacobsen et al. 2007, Ziemińska et al. 2013, 2015, Fortunel et al. 2014, Plavcová et al. 2019). Such investigations have, however, been rare for parenchyma, limiting our understanding of the physiological significance of variations in parenchyma. Clarifications of this could explain why parenchyma fraction varies greatly among species (Fichtler and Worbes 2012, Spicer 2014) and with climate (Morris et al. 2016*b*, Zheng et al. 2019).

Parenchyma fraction within xylem sapwood potentially influences xylem functions in several ways. On one hand, parenchyma cells store starch as storage carbohydrates within the sapwood and provide soluble sugars as osmolytes and as substances for the respiration, transportation and synthesis of other molecules to maintain cell metabolism (Spicer and Holbrook 2007, Hartmann and Trumbore 2016, Saiki et al. 2017). Thus, parenchyma fraction would directly regulate the storage capacity of soluble sugars and starch within the xylem sapwood. Supporting the latter, investigations in temperate regions have revealed significant positive associations between the parenchyma fraction and concentrations of starch and NSC across species (Plavcová et al. 2016, Chen et al. 2020, Pratt et al. 2021). On the other hand, increases in the parenchyma fraction decrease the space occupied by fibers and vessels (Morris et al. 2016*b*). This negative correlation would give rise to trade-offs among storage capacity, water conduction and mechanical strength among species (Pratt and Jacobsen 2017). Previous studies have shown that a high fraction of parenchyma is associated with a low wood density and a low bulk modulus of elasticity in xylem sapwood (Jacobsen et al. 2007, Pratt et al. 2007, Fortunel et al. 2014). However, many studies have evaluated only one plausible function of parenchyma (e.g., storage of carbon and water). Thus, our understanding of how parenchyma fraction translates into xylem multiple functions (e.g., water conduction, storage and mechanical strength) directly or indirectly via interactions with other xylem components remains limited (but see Pratt et al. 2007, Plavcová et al. 2019).

The functional significance of parenchyma may differ among cell types. Parenchyma generally consists of two types: axial parenchyma (AP) and ray parenchyma (RP), which have a different development and connectivity to other tissues and cells (Spicer 2014). Both AP and RP show different correlation patterns with wood density, vessel traits (Zheng and Martínez-Cabrera 2013, Morris et al. 2018*a*) and climate (Martínez-Cabrera et al. 2009, Zheng et al. 2019). In addition, the morphologies of AP, such as pit structures, are different between the AP in direct contact with the vessels (APV) and those without vessels (Morris et al. 2018*b*). The APV is also characterized by high physiological activities, particularly during drought, including the active regulation of pH in xylem sap (Fromard et al. 1995) and, possibly, the recovery of embolized vessels (Brodersen and McElrone 2013, Knipfer et al. 2016, Secchi et al. 2017) and surfactant production (Schenk et al. 2017). Morris et al. (2018*a*) qualitatively and quantitatively demonstrated that xylem with large vessels was associated with a high fraction of AP, suggesting that AP is involved in the maintenance of hydraulic conductivity. Supporting the latter, the close associations between the hydraulic properties of xylem and AP and APV are being increasingly demonstrated: xylem with high fractions of AP and APV is associated with high conductivity and low resistance to cavitation across a wide range of species (Kiorapostolou et al. 2019, Chen et al. 2020, Janssen et al. 2020, but see Aritsara et al. 2021). It has also been reported that a higher vessel-AP contact fraction is associated with greater hydraulic capacitance (Ziemińska et al. 2020) and potentially facilitates the refilling process through the osmotically driven influx of water to embolized vessels, although this is controversial (Salleo et al. 2004, Secchi and Zwieniecki 2012, Yoshimura et al. 2016, Secchi et al. 2017). These findings suggest that the parenchyma fraction underpins the trade-offs among the hydraulic properties of xylem (e.g., cavitation resistance and capacitance, Gleason et al. 2016*b*). However, few studies have quantified species variation in AP and APV or examined their linkages to xylem hydraulic properties, especially in field-grown trees.

In the present study, using the sapwood from branches of 15 drought-adapted co-occurring woody species from a subtropical oceanic island, we examined the coordination between parenchyma fraction and three xylem functions (i.e., hydraulic properties, carbon storage and mechanical strength). We assessed the hydraulic properties of sapwood using three water relations: the maximum hydraulic conductivity, the degree of embolism and the xylem water potential at midday (XWP). The carbon storage of sapwood was examined based on the concentrations of NSC (Chapin et al. 1990). The mechanical strength of sapwood was assessed by sapwood density, based on its strong association with fracture toughness and stiffness (Young's modulus) of wood across species (van Gelder et al. 2006, Alvarez-Clare and Kitajima 2007, Jacobsen et al. 2007, Chave et al. 2009, Méndez-Alonzo et al. 2012). The studied island, one of the Bonin Islands in Japan, commonly experiences relative soil droughts during the summer and this trend is often strengthened by interannual variations in rainfall seasonality (Yoshida and Iijima 2009). Thus, summer droughts may influence the xylem anatomy of woody plants on this island in the long term (Ishida et al. 2008), as in other subtropical islands (Dória et al. 2018). Based on the associations between parenchyma and vessels (Zheng and Martínez-Cabrera 2013, Morris et al. 2018*a*, Janssen et al. 2020), NSC storage (Plavcová et al. 2016, Chen et al. 2020, Pratt et al. 2021),

and sapwood density (Jacobsen et al. 2005), we hypothesized that: (i) both vessels and parenchyma (particularly APV which is directly connected to vessels) are related to xylem hydraulic properties, and that a high fraction of parenchyma leads to (ii) high concentrations of soluble sugars and starch and (iii) a low wood density because of the low fractions of vessels and fibers.

Materials and methods

Study site and plant species

This study was conducted on Chichi-jima Island (27°04′N, 142°13′E; maximum elevation of 318 m a.s.l.), one of the Bonin (Ogasawara) Islands located in the northwest Pacific Ocean. This island is a subtropical oceanic island, ∼1000 km south of Tokyo, Japan, and is authorized as a World Natural Heritage site. The mean annual temperature and mean annual precipitation from 2009 to 2018 were 23.4 °C and 1281 mm, respectively (Japan Meteorological Agency). Seasonal drought usually occurs in the summer months (July–September) as a result of the development of the North Pacific High (Yoshida and Iijima 2009). In addition, interannual variations in climate often strengthen this trend in several-years cycle. For example, in 2016 and 2020, the level of precipitation from June to August was 42 to 56% of the average during 1999–2018, respectively, despite similar temperatures (Japan Meteorological Agency). In 2020, the predawn and midday leaf water potential showed relatively low values during summer: −3.0 and −4.2 MPa, respectively, for *Rhaphiolepis integerrima*—a dominant woody species (our unpublished data). The minimum temperature does not fall below 0 °C; thus, freezing is not an evolutionary driver of xylem anatomy (e.g., Zanne et al. 2014).

We chose co-occurring 15 drought-adapted and native woody species comprising 12 families in a dry dwarf forest (see Table S1 available as Supplementary data at *Tree Physiology* Online). Many endemic tree species are predominant in ridge areas with shallow soil on the island (Shimizu 1992). Among the examined species, *Dodonaea viscosa, Osmanthus insularis, Photinia wrightiana*, and *Rhaphiolepis integerrima* are indigenous to Japan, and the other 11 species are endemic to the Bonin Islands. Three to four healthy adult trees that ranged from 1.0 to 8.0 m in height and received direct sunlight at the canopy were selected for each species. All studied individuals were found in places with similar topographic conditions, which were at most 1 km apart. All tree species had similar growth forms (i.e., broad-leaved evergreen trees). Plant nomenclature followed the 'Japanese name-scientific names index' (Yonekura and Kajita 2003, available online at http://ylist.info/, accessed 13 April 2020). In total, 17 xylem traits were measured for each species (Table 1). To capture the anatomical tuning to dry summer, we measured the physiological properties of xylem in the summer.

Xylem hydraulic properties

We measured the xylem hydraulic conductivity, percentage loss of conductivity (PLC) and XWP at midday from July 3rd to August 3rd in 2019. The study year (2019) was a relatively less-dry year. The average daily air temperature, total precipitation, vapor pressure deficit during midday (from 10:00 to 16:00 h) and volumetric soil water content, which were measured near the sampled trees during the measurements, were 29.9 °C, 1.05 mm, 1.20 kPa and 0.32 m^3 m^{-3}, which were the highest, lowest, highest and the third lowest among the monthly averaged values from 2019 July to 2020 June, respectively (our unpublished data). These relatively dry conditions in July were also recorded during 1999–2018 (Japan Meteorological Agency). Thus, we consider that the hydraulic properties were measured during the most seasonal desiccating period on this island.

For stem hydraulic efficiency, we measured one to three sunlit branches for each individual tree (n = 4–7 per species). Branches of ∼1 m in length were collected before dawn (04:30–06:00 h) and immediately re-cut under water. The branches were then immediately transported to the laboratory with the cut ends submerged in water where they were enclosed in black plastic bags for at least 2 h to relax the xylem tension. Using the method of Sperry et al. (1988), we measured the hydraulic conductivity in the longest branch segments without any side branches (the length and diameter of all samples ranged from 8 to 48 cm with a mean value of 22 cm and from 4 to 13 mm with a mean value of 8 mm, respectively). After gently removing the bark at both ends, the branch sample was connected to the tubing system, and a hydraulic pressure of approximately 5 kPa was applied to the end of the segments by locating the water bag containing 20-mM KCl solution to *c.* 50-cm height from the sample. The other end was connected to a plastic bottle on an electronic balance using a tube, and the water flow rate from the segment was automatically measured. The water flow rate was divided by the pressure per unit length of the segment to obtain the initial xylem hydraulic conductivity ($K_{initial}$). Subsequently, the same segment was flushed with 20-mM KCl solution under 0.15 MPa for 10 min to remove air-induced xylem embolism, and the water-flow rate was measured again to yield the maximum xylem hydraulic conductivity ($K_{flushed}$). The KCl solution was filtered to 0.2-μm pore diameter using a vacuum pump before the measurements. All measurements were performed at a constant temperature of 26 °C. The PLC was calculated as follows:

$$PLC = \left(1 - \frac{K_{initial}}{K_{flushed}}\right) \times 100 \quad (1)$$

We note two concerns regarding the above methods. The first is the overestimation of PLC by the introduction of air to open vessels when cutting stems in the air ('excision artifact',

Table 1. Xylem traits studied, including the minimum species mean, mean of species mean, maximum species mean and standard error (SE) for 15 woody species in the Bonin Islands, Japan.

Trait	Abbreviation	Unit	Mean (SE)	Min	Max
Xylem water potential at midday	XWP	MPa	−1.21 (0.10)	−1.87	−0.56
Xylem-area specific conductivity[a]	K_{max}	kg m^{-1} s^{-1} MPa^{-1}	1.2 (0.2)	0.5	3.4
Percentage loss of conductivity[b]	PLC	%	14.5 (2.7)	4.0	43.2
Volume-based soluble sugar concentration	SS_v	mg cm^{-3}	16.2 (1.5)	7.0	27.3
Volume-based starch concentration	ST_v	mg cm^{-3}	24.2 (3.9)	6.4	56.5
Volume-based concentration of soluble sugars and starch	T_v	mg cm^{-3}	40.4 (4.3)	14.6	75.5
Sapwood density	WD	g cm^{-3}	0.69 (0.03)	0.52	0.83
Fraction of vessels in transverse section[b]	F_v	–	0.097 (0.011)	0.049	0.227
Fraction of fibers in transverse section	F_f	–	0.675 (0.016)	0.557	0.777
Fraction of total parenchyma in transverse section	F_p	–	0.227 (0.020)	0.112	0.391
Fraction of axial parenchyma in transverse section	F_{ap}	–	0.075 (0.015)	0.008	0.215
Fraction of ray parenchyma in transverse section[b]	F_{rp}	–	0.153 (0.012)	0.093	0.262
Fraction of axial parenchyma in direct contact with vessels (APV) in transverse section	F_{apv}	–	0.023 (0.003)	0.003	0.038
Vessel density	VD	mm^{-2}	240 (36)	74	486
Mean hydraulically weighed vessel diameter[a]	D_h	mm	0.027 (0.002)	0.018	0.047
Potential hydraulic conductivity[a]	K_p	kg m^{-1} s^{-1} MPa^{-1}	3.0 (0.7)	1.1	8.6
Potential resistance to vessel implosion	RI	–	0.051 (0.007)	0.016	0.116

[a]Log_{10}-transformed before analysis.
[b]Logit-transformed before analysis.
For each species' trait data, see Table S1 available as Supplementary data at *Tree Physiology* Online.

Wheeler et al. 2013). However, the predawn leaf water potential when we collected stems was relatively high (> −0.7 MPa, our unpublished data) and the maximum vessel length for most of our studied species (shrub or dwarf tree) would be relatively short (Jacobsen et al. 2012). Thus, this bias would be minimal (Torres-Ruiz et al. 2015). In addition, it was not realistic to sample enough long stems due to the stature of the trees and legal restrictions (the study area is authorized as a World Natural Heritage site). The second concern is the underestimation of PLC by a relatively long relaxation time for xylem tension (e.g., Trifilò et al. 2014, Venturas et al. 2015). However, because our relaxation time did not vary much among samples, we considered the relative comparison among species to be still possible and meaningful.

After the measurements, the images of the sapwood cross-section at both ends were obtained using a digital microscope (Dino-Lite, AnMo Electronics Corporation, Taipei, Taiwan), and the cross-sectional area of xylem sapwood (A_s) was measured with image processing software, Fiji (Schindelin et al. 2012).The value of $K_{flushed}$ was divided by A_s to obtain the xylem-area specific conductivity (K_{max}).

The XWP was measured with a Scholander-type pressure chamber (PMS Instrument Company, Albany, OR, USA). On the day before the measurement, several leaves per individual were covered with a thin film of polyvinyl chloride and aluminium foil to prevent water loss by transpiration and allow the leaf water potential to equilibrate with the XWP. On the following day, the wrapped leaves were collected from 10:00 to 12:30 h on sunny days and were immediately stored in a dark cooler box. The samples were immediately transported to the laboratory, where-after the leaf water potential was measured for at least two leaves per individual, assuming that the values of the leaf water potential were in equilibrium with those of the XWP in the branches when we collected them during the daytime.

NSC storage within sapwood

The concentrations of soluble sugars, starch and their sum were measured in different stem segments to calculate K_{max} and PLC in the same branches. We assumed that the sum of soluble sugars and starch accounted for most of the sapwood NSC for woody species (Hoch et al. 2003). Based on our preliminary observations using the same woody species, we also assumed that the NSC levels are highest during summer because summer droughts would constrain growth more than photosynthesis, resulting in the accumulation of carbon reserves, as in other tropical (Würth et al. 2005) and subtropical (Liu et al. 2018) regions during the dry season. After we collected the samples in the field, they were immediately transported to the laboratory in a dark cooler box, followed by the swift removal of bark before oven drying (65 °C, >72 h). After drying, the pith was removed, and the remnants were ground to a fine powder using a mill, followed by extraction in 80% (v/v) ethanol three times. The supernatant was extracted via centrifugation (15,000 rpm for 10 minutes for first and second extractions and 30 minutes for third one) and used to quantify the soluble sugar content via the phenol–sulfuric acid method (Dubois et al.

1951). The starch in the remaining pellets was depolymerized to glucose by amyloglucosidase, and the content was quantified using the mutarotase–glucose oxidase method (Glucose C-II test; Wako, Tokyo, Japan). The mass-based concentrations were transformed to volume-based concentrations by multiplying the sapwood density for each individual. Because most anatomical traits are measured in linear dimensions, they are expected to be strongly related to variables with volume dimensions rather than those with different dimensions (e.g., kilograms). Consistent with Pratt et al. (2021), both mass- and volume- basis expressions were strongly correlated with each other across species ($r = 0.87$, $r = 0.95$, $r = 0.89$, for soluble sugars, starch and the total sum of them, respectively), due to a relatively narrow range of sapwood density across species compared with NSC concentration. Thus, the confounding effect of sapwood density was small, and our conclusion was robust regardless of the method of standardization (see also Results section).

Sapwood density

The sapwood density was measured for one branch per tree. Stem segments with lengths of approximately 1 cm and with similar diameters for measurements of K_{max} and PLC were collected, and their bark was removed. The sapwood volume was estimated by assuming a cylindrical shape with a digital caliper, and their dry mass was weighed after oven-drying (65 °C, > 72 h). The sapwood density was obtained by dividing the dry mass by its fresh volume.

Xylem anatomy

Using one branch per tree ($n = 3$ per species), we measured 10 xylem anatomical traits (Table 1). After the hydraulic measurements, the central part of the stem segment (approximately 1 cm in length) was collected and chemically fixed in 3% (v/v) glutaraldehyde before analysis. Transverse sections of ~30–40-μm thickness were prepared using a sliding microtome. Samples were double-stained with 1.0% (w/v) alcian blue (in 3% acetic acid) and 0.5% (w/v) safranin (in 50% ethanol) and dehydrated using an ethanol series (50, 99.5 and 100%). Finally, the samples were dehydrated in xylene and mounted on glass slides with Canada balsam. Photographic images were captured with a 10× objective using a light microscope (BX50, Olympus, Tokyo, Japan) and a digital camera (EOS kiss X3, Canon, Tokyo, Japan).

The fractions of vessels (F_v), fibers (F_f), total parenchyma (F_p), axial parenchyma (F_{ap}), ray parenchyma (F_{rp}) and AP in direct contact with vessels (F_{apv}) in the xylem transverse section were measured in a rectangular region (*c.* 1 mm^2) located at the middle position from the pith to the cambium, avoiding reaction wood. The resolution of the image was 1919 pixels per millimeter with a full extent of *c.* 1.2 mm × 0.8 mm. In each image, we manually filled the different types of parenchyma, including their cell walls, with different colors in Pixelmator ver. 2.4.8. (Pixelmator Team, Vilnius, Lithuania). In case of ambiguity between cell types, we consulted an expert in woody anatomy to confirm the identification (Yuzou Sano, personal communication). The area of each cell type was measured using Fiji, yielding F_{ap}, F_{rp} and F_{apv}. The F_p was calculated as $F_{ap} + F_{rp}$. Then, we manually filled the vessels in the same image using GIMP ver. 2.8.18 (www.gimp.org), and their area was measured using Fiji, yielding F_v. Finally, we calculated F_f as 1—F_p—F_v. In the present study, we focused on APV and not RP in direct contact with vessels (RPV) or contact cells (the sum of APV of RPV, Morris and Jansen 2016, Morris et al. 2018*b*) due to the following reasons: (i) our interest was in the interspecific differences in AP, and (ii) neither fractions of RPV nor CC, which were highly positively correlated with each other ($r = 0.92$ and $P < 0.001$), were significantly correlated with any xylem traits examined (data not shown). In addition, although vessel-distant AP in direct contact with APV may function as a continuum, this was not considered in the present study because it is unclear for the scale of AP around vessels functioning together for different species.

Using the same image, we measured the vessel density (VD), mean hydraulically weighted vessel diameter (D_h), potential xylem hydraulic conductivity (K_p) and potential resistance to vessel implosion (RI). The VD values were calculated as the number of vessels divided by the area of the analyzed region. The values of D_h were calculated as follows (Tyree and Zimmermann 2002):

$$D_h = \sqrt[\frac{1}{4}]{\frac{1}{n}\sum_{i=1}^{n} d^4} \quad (2)$$

where d is the diameter of each vessel. Because a vessel cross-section is not exactly a circle, d was calculated as the average of the mean length of the major and minor axes of the ellipse fitted to each vessel. Using VD and D_h, we calculated K_p as follows (Poorter et al. 2010):

$$K_p = \frac{\pi \rho_w}{128\eta} \text{VD } D_h^4 \quad (3)$$

where ρ_w is the density of water at 20 °C (998.2 kg m^{-3}), and η is the viscosity of water at 20 °C (1.002 × 10^{-3} Pa s). Note that K_p is higher than K_{max} because K_p does not consider the flow resistance through the intervessel pit pores and the three-dimensional network of xylem, which typically account for > 50% of the total resistance of the vessel network (Schulte et al. 1987, Wheeler et al. 2005, Loepfe et al. 2007, Choat et al. 2008).

As an index of xylem cavitation resistance, we calculated the vessel resistance to implosion (RI) as $(t/b)^2$, where t is the double-wall thickness of adjacent vessels and b is the span of the vessel lumen (Hacke et al. 2001). The values of t and b were measured on at least 15 vessel pairs per individual that averaged within 40% of D_h, using Fiji. The values of b were

estimated as the side of the square with an area equal to the average vessel lumen.

Statistical analysis

All analyses were performed using R (version 3.6.1; R core Team 2019). We calculated the mean trait values for each species, and some trait values were transformed to improve the normality and reduce the heteroscedasticity of the residuals in linear regressions (Table 1). Traits ranging in (0, ∞) were $\log_{10}$-transformed, whereas traits ranging in a limited range (e.g., percentage or fraction data) were expressed in the proportional range [0, 1] and then logit-transformed before analyses (Warton and Hui 2011). For PLC, we added the minimum non-zero PLC values (*c.* 0.24%) to both the numerator and denominator of the logit function before transformation, as recommended by Warton and Hui (2011). First, we examined the hypothesized relationships using Pearson's product–moment correlation. When a significant correlation ($P < 0.05$) was observed, the line was fitted by standard major axis using the R package 'smatr' (Warton et al. 2012). We also evaluated the impact of phylogenetic relationships for pairwise trait correlations using phylogenetically independent contrasts (PICs, Felsenstein 1985) using the R package 'ape' (Paradis et al. 2004). PHYLOMATIC (ver. 3) (Webb and Donoghue 2005; available online at http://www.phylodiversity.net/phylomatic/) was used to build the tree for the studied species based on megatree by Slik and Franklin (2018), assuming an equal branch length of 1 to avoid uncertainty in phylogenetic distances among closely related species (Ackerly 2000).

To clarify the multiple correlation patterns in xylem traits, we conducted a principal component analysis (PCA). We also conducted path analysis using the R package 'lavaan' (Rosseel 2012) to infer the potential causal relationships between xylem anatomy (parenchyma and vessel) and functions. This analysis was based on our hypotheses and bivariate trait correlations. The overall model fit was assessed with a X^2-test, where non-significance ($P > 0.05$) indicated failure to reject the model. Alternative plausible models were generated through the addition and subtraction of variables, and the model with the lowest Akaike Information Criterion (AIC) with significant paths was selected.

Results

The 15 drought-adapted woody species from a subtropical oceanic island showed markedly different xylem traits in terms of anatomy and function (Table 1; see Table S1 and Figure S1, available as Supplementary data at *Tree Physiology* Online). The fraction of AP (F_{ap}) varied 27.4-fold (0.008–0.215), that of AP in direct contact with vessels (F_{apv}) varied 11.6-fold (0.003–0.038), the PLC varied 11.0-fold (4.0–43.2%) and volume-based starch concentration (ST_v) varied by 8.9-fold (6.4–56.5 mg cm^{-3}) among the tree species. The interspecific variation in the fraction of RP (F_{rp}, 2.8-fold) was smaller than that of F_{ap}, but the mean value of the F_{rp} was higher than that of F_{ap} (0.153 ± 0.012 and 0.075 ± 0.015, respectively; paired *t*-test, $P = 0.001$), accounting for 36–95% of the fraction of parenchyma (F_p). The mean value of F_{apv} was lower than that of the vessel-distant AP (0.023 ± 0.003 and 0.052 ± 0.014, respectively; paired *t*-test, $P = 0.03$), accounting for an average of 41% of F_{apv}. The F_{apv} increased with F_{ap} across species but plateaued after F_{ap} exceeded ∼0.1 (see Figure S2 available as Supplementary data at *Tree Physiology* Online), resulting in a decreased percentage of paratracheal AP in the total AP. We observed many significant hypothesized correlations among traits and these results were qualitatively and quantitatively similar to those using phylogenetically independent contrasts (PICs, Table 2). Thus, the relationships between xylem anatomy and functions for the studied species would be due to correlated evolution at multiple nodes, rather than changes within a few nodes.

Relationships of parenchyma with xylem functions

Consistent with hypothesis (1), both vessel and parenchyma traits showed significant correlations with xylem hydraulic properties, except for XWP at midday. The xylem-area specific conductivity (K_{max}) was positively associated with vessel fraction (F_v, Figure 1a) and potential hydraulic conductivity (K_p), but negatively associated with F_{rp} (Figure 1c). PLC was significantly and positively correlated with the hydraulically weighted vessel diameter (D_h) and negatively correlated with VD (Figure 1f, $r = 0.54$, $P = 0.04$; $r = -0.62$, $P = 0.01$). PLC was positively associated with F_{ap} and F_{apv}, with the latter being stronger (Figure 1h, Table 2). The XWP values were positively correlated with D_h and K_p across species (Table 2).

Significant correlations were found between the fraction of parenchyma and vessel morphology (fraction, density and diameter) and the correlation patterns were slightly different among parenchyma types (Table 2): F_{rp} was negatively correlated with K_p, whereas F_{ap} and F_p were negatively correlated with F_v and VD. F_{apv} was negatively correlated with VD and positively correlated with D_h.

Slightly different from hypothesis (2), the parenchyma fraction was positively associated with the concentration of starch (ST_v), whereas it was not significantly correlated with that of soluble sugars. The ST_v was marginally and positively correlated with F_{rp}, F_p (Figure 2a), and vessel resistance to implosion (RI), whereas it was negatively correlated with F_v (Table 2). The F_{ap} was also significantly correlated with ST_v when *Ligustrum micranthum*, which showed a high ST_v and a low F_{ap}, or *Syzygium cleyerifolium*, which showed a low ST_v and a high F_{ap}, were removed (Figure 2b, $r = 0.54$, $P < 0.05$ for both relationships for 14 species). The concentration of soluble sugars (SS_v) was

Table 2. Pearson's correlation coefficients among the 17 xylem traits for 15 woody species in the Bonin Islands, Japan

	XWP	K_{max}[a]	PLC[b]	SS_v	ST_v	T_v	WD	F_v[b]	F_f	F_p	F_{ap}	F_{rp}[b]	F_{apv}	VD	D_h[a]	K_p[a]	RI
XWP		0.31	0.12	−0.46†	0.11	−0.07	−0.41	0.11	−0.50†	0.29	**0.57**	−0.28	0.20	−0.45†	**0.75**	**0.54**	−0.28
K_{max}[a]	0.26		−0.37	−0.35	−0.47†	**−0.55**	−0.37	**0.81**	−0.16	**−0.57**	−0.25	**−0.72**	−0.27	0.32	0.32	**0.71**	**−0.53**
PLC[b]	0.20	−0.23		−0.23	0.47†	0.34	0.33	−0.44†	**−0.52**	**0.64**	**0.63**	−0.33	**0.74**	**−0.59**	0.35	0.06	−0.08
SS_v	−0.40	−0.39	−0.19		0.08	0.44	0.49†	−0.23	0.39	−0.17	−0.28	0.11	−0.31	**0.52**	**−0.74**	**−0.63**	**0.72**
ST_v	0.10	−0.49†	0.10	0.13		**0.93**	0.39	−0.39	−0.44†	**0.54**	0.40	0.46†	0.38	−0.20	0.01	−0.24	0.51†
T_v	−0.05	**−0.58**	0.02	0.47†	**0.94**		**0.53**	−0.43	−0.26	0.42	0.26	0.45†	0.22	−0.01	−0.26	−0.45†	**0.73**
WD	**−0.52**	−0.31	0.02	**0.60**	0.26	0.44†		−0.43	0.03	0.24	0.19	0.23	−0.00	0.18	−0.50†	**−0.61**	**0.69**
F_v[b]	0.07	**0.77**	−0.31	−0.36	−0.48†	**−0.55**	−0.41		0.21	**−0.67**	**−0.52**	**−0.55**	−0.37	**0.59**	0.22	**0.76**	−0.47†
F_f	−0.37	−0.01	−0.28	0.40	−0.29	−0.12	0.07	0.09		**−0.85**	**−0.77**	−0.49†	**−0.53**	0.41	−0.36	−0.08	0.21
F_p	0.21	−0.45†	0.39	−0.11	0.50†	0.41	0.18	**−0.63**	**−0.82**		**0.84**	**0.69**	**0.60**	**−0.61**	0.16	−0.33	0.08
F_{ap}	0.39	−0.15	**0.52**	−0.17	0.32	0.23	0.11	**−0.55**	**−0.66**	**0.81**		0.20	**0.69**	**−0.71**	0.44	0.07	0.04
F_{rp}[b]	−0.24	**−0.59**	−0.04	0.10	0.45†	0.43	0.23	−0.38	−0.48†	**0.62**	0.04		−0.19	0.15	−0.33	**−0.55**	0.25
F_{apv}	0.10	−0.11	**0.67**	−0.31	0.18	0.05	−0.14	−0.31	−0.45†	**0.53**	**0.73**	−0.07		**−0.71**	0.46†	0.06	−0.21
VD	−0.44	0.23	**−0.62**	0.41	−0.23	−0.06	0.31	**0.53**	0.33	**−0.54**	**−0.73**	0.06	**−0.78**		**−0.61**	−0.05	−0.17
D_h[a]	**0.64**	0.25	**0.54**	**−0.62**	0.00	−0.22	**−0.61**	0.09	−0.28	0.16	0.47†	−0.39	**0.64**	**−0.77**		**0.80**	−0.45†
K_p[a]	**0.54**	**0.59**	0.26	**−0.67**	−0.24	−0.45†	**−0.72**	**0.59**	−0.14	−0.23	0.06	**−0.52**	0.34	−0.34	**0.85**		**−0.58**
RI	−0.22	−0.51†	−0.03	**0.66**	**0.61**	**0.78**	**0.60**	**−0.62**	0.20	0.19	0.14	0.21	−0.04	−0.06	−0.24	−0.50†	

Pearson correlation coefficients are shown below the diagonal, and above the diagonal for phylogenetically independent contrast (PIC) correlations. Significant correlations are indicated by bold ($P < 0.05$) and underlined bold ($P < 0.01$). †$0.05 \leq P < 0.10$.
[a]Log_{10}-transformed before analysis.
[b]Logit-transformed before analysis.
For trait abbreviation, see Table 1.

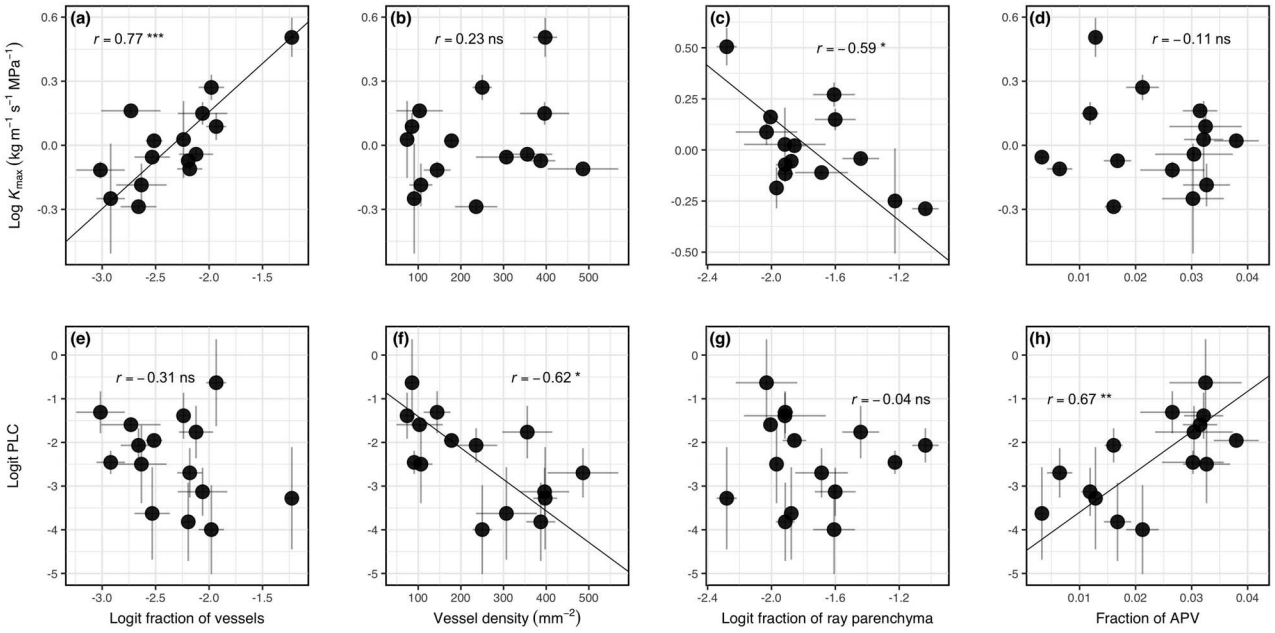

Figure 1. Relationships between xylem hydraulic properties and vessel and parenchyma traits. The xylem-area specific conductivity (K_{max}) against (a) the fraction of vessel, (b) VD, (c) fraction of RP and (d) fraction of AP in direct contact with vessels (APV). The PLC against (e) fraction of vessel, (f) VD, (g) fraction of RP and (h) fraction of APV. Some proportional variables were logit-transformed (unitless; see Materials and methods). Error bars represent 1 standard error (SE). Lines were fitted by the standard major axis. ***$P < 0.001$; **$P < 0.01$ and *$P < 0.05$, ns: not significant.

positively correlated with RI and negatively correlated with D_h and K_p (Table 2). Reflecting the above trends, the concentration of soluble sugars and starch (T_v) positively co-varied with RI and negatively with F_v and K_p. Except for *L. micranthum*, which showed the highest T_v among species, F_{ap}, F_{rp} and F_p were positively correlated with T_v ($r = 0.52$, $P = 0.06$; $r = 0.49$, $P = 0.08$; $r = 0.67$, $P = 0.009$, respectively, for 14 species). We obtained similar, but less significant results even when using mass-based concentration of NSC, indicating the robustness of our results regardless of the method of standardization (for the relationships with parenchyma fraction, see Figure S3 available as Supplementary data at *Tree Physiology* Online).

In contrast to hypothesis (3), although F_p was negatively correlated with the fractions of vessels and fibers, none of them correlated with sapwood density (WD, Figure 3a and Table 2). Independence of WD was found for F_{ap}, F_{rp} and

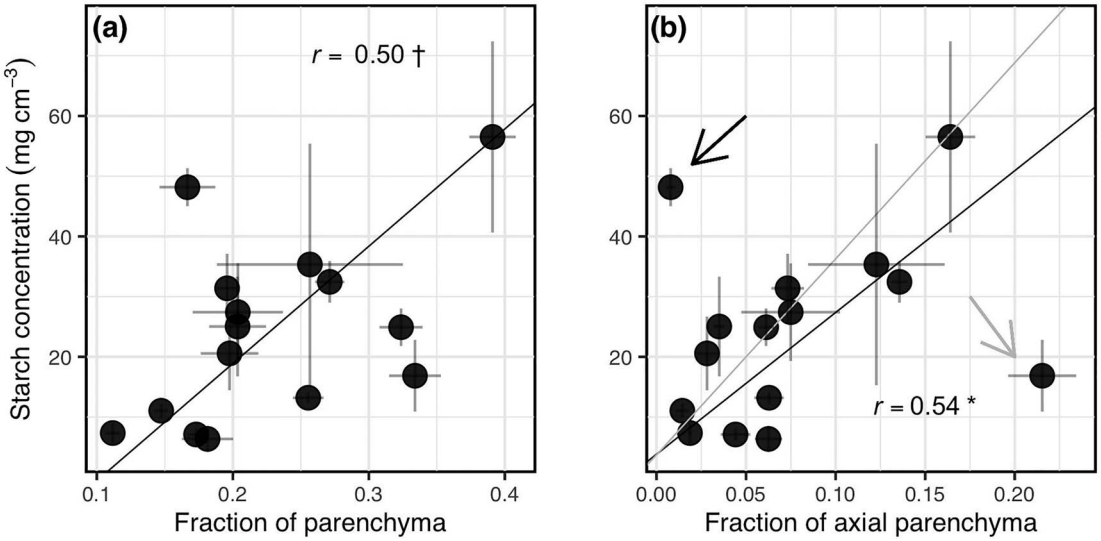

Figure 2. Relationships between starch concentration and the fractions of (a) parenchyma and (b) AP. Error bars represent 1 standard error (SE). Lines were fitted by the standard major axis. In (b), the line represents trends without *Ligustrum micranthum* (denoted by a black arrow) or *Syzygium cleyerifolium* (denoted by a gray arrow), corresponding to the black and gray line, respectively. $^{*}P < 0.05$; $^{\dagger}0.05 \leq P < 0.10$.

F_{apv}. The values of WD were positively correlated with RI and negatively correlated with D_h and K_p across species (Figure 3b and Table 2).

In the PCA for the 17 traits and 15 species, the first and second axes accounted for 64.4% of the total variation (Figure 4). The results summarized the above correlations among the xylem anatomy and functions across species. The first axis explained 33.2% of the variation, showing positive loadings for K_{max}, F_v, D_h and K_p and negative loadings for SS_v, ST_v, T_v, WD, F_{rp}, RI (all $P < 0.05$, Pearson's correlation between scores in PCA axis and each trait among species) and F_p ($P = 0.05$). The second axis explained 31.2% of the variation, showing positive loadings for XWP, PLC, F_p, F_{ap}, F_{apv} and D_h and negative loadings for F_f, VD (all $P < 0.05$) and SS_v ($P = 0.07$).

Path analysis confirmed that fractions of axial and RP were significantly related to PLC, maximum hydraulic conductivity (K_{max}) and starch storage across species (Figure 5). The model predicted that the fraction of AP increases PLC and that of RP reduces K_{max}, whereas both fractions increase starch storage. Negative covariances between the fractions of vessel and parenchyma must be included for the model fit. Adding hydraulically weighted vessel diameter (D_h) to this model with an insignificant path to PLC significantly reduced the model fit ($X^2 = 24.3$, $P = 0.04$ and $\Delta AIC = 48.9$). Furthermore, substituting D_h for F_{ap} with no path form D_h to starch storage and with covariances of D_h with F_{rp} and F_v reduced the model fit ($X^2 = 7.5$, $P = 0.58$ and $\Delta AIC = 2.7$). When removing *L. micranthum*, which showed a high starch storage and a low F_{ap}, the path from F_{ap} to starch storage became significant. Similar results were obtained even when using the mass-based concentration of NSC (data not shown).

Discussion

Coordination between parenchyma and stem hydraulics

Long-distance water transport in trees has long been thought to be regulated by dead vessels (e.g., Tyree and Zimmermann 2002, Sperry et al. 2006). However, recent studies have increasingly emphasized the role of living cells in the dynamic regulation of xylem water transport (Salleo et al. 2004, Scoffoni and Sack 2017, Secchi et al. 2017, Morris et al. 2018*a*). In the present study, we showed that the fraction of RP was negatively correlated with xylem hydraulic efficiency (K_{max}), whereas that of AP and AP in direct contact with vessels (APV) was positively associated with the native cavitation level (Figures 1 and 5 and Table 2). With regard to the former, although not significant in correlation analysis not using PICs (Table 2), the increase fraction in RP may decrease that of vessels, thereby reducing K_{max}. A similarly negative association between RP fraction and K_{max} was previously reported in Magnoliids (Aritsara et al. 2021).

For the positive relationship between PLC and AP or APV, given the relatively narrow range of XWP (−1.87 to −0.56 MPa, Table 1) and large differences in cavitation resistance among the species studied (Yoshimura et al. 2016 and our unpublished data), we speculate that xylem with high fractions of AP or APV is susceptible to drought-induced xylem embolism. Although small vessels associated with high fractions of AP or APV (Table 2, Morris et al. 2018*a*) also confer cavitation resistance in some cases (Hacke et al. 2017), the results of our path analysis (Figure 5) suggest that AP or APV affect PLC more than vessel diameter. A negative association between fractions of AP or APV with cavitation resistance was recently reported

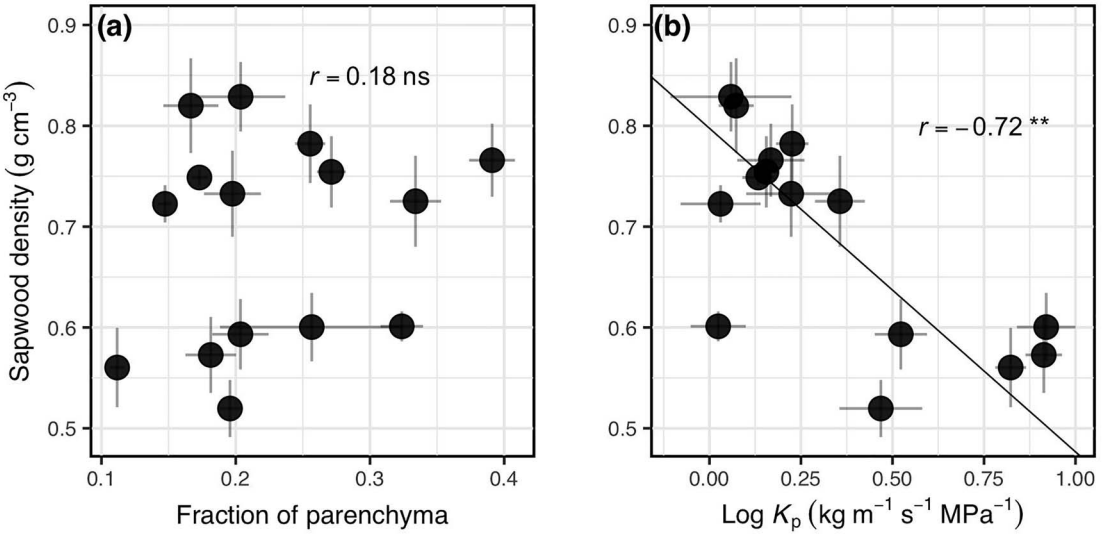

Figure 3. Relationships between sapwood density and (a) the fraction of parenchyma and (b) potential hydraulic conductivity (K_p). Error bars represent 1 standard error (SE). The line was fitted by the standard major axis. $^{**}P < 0.01$; ns: not significant.

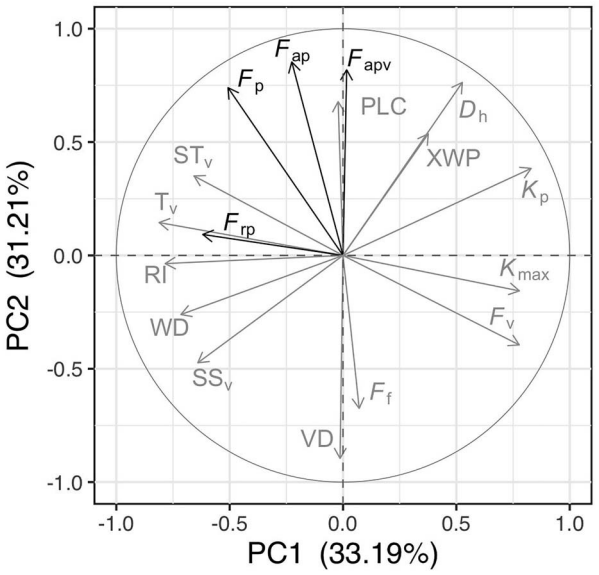

Figure 4. Principal component analysis for the 17 xylem traits of 15 woody species in the Bonin Islands, Japan. Numbers in parentheses represent the percentage of variance explained by each axis. Parenchyma traits are shown in black arrows while other xylem traits are shown in gray arrows. See Table 1 for trait abbreviations.

(Kiorapostolou et al. 2019, Chen et al. 2020, Janssen et al. 2020). However, positive associations have also been reported in some mesic tree species (Aritsara et al. 2021).

A possible mechanism for the negative relationship between AP and cavitation resistance is that species with high fractions of AP or APV utilize different drought tolerance strategies, which may compromise drought-resistant strategies (Gleason et al. 2016*b*, Chen et al. 2020). These strategies include a cavitation avoidance strategy through enhanced capacitance (Ziemińska et al. 2020) and an embolism repair strategy possibly through the deposition of soluble sugars from APV (Secchi and Zwieniecki 2012).

The positive linkage between AP or APV and embolism repair capacity is partially supported in our previous study on this island. Yoshimura et al. (2016) monitored the hydraulic conductivity and concentration of NSC of branch xylem during dehydration and rehydration periods in summer, using *Hibiscus glaber* with a high APV fraction and low cavitation resistance and *L. micranthum* with a low APV fraction and high cavitation resistance. *H. glaber* showed higher cavitation levels than *L. micranthum* during the dehydration period, but showed a greater recovery in hydraulic conductivity, with water supply following starch conversion to soluble sugars, which was not observed in *L. micranthum*. Thus, high fractions of AP or APV may be important for facilitating embolism recovery under ample starch storage. Future studies should demonstrate this prediction and also clarify why this strategy is mechanistically associated with low cavitation resistance. Based on the high physiological activities of APV, which should be associated with high respirational cost, carbon allocation to structural (e.g., fiber and vessel cell walls for high cavitation resistance) and non-structural components (e.g., starch storage in APV for embolism repair) in the xylem may be relevant in this trade-off.

Coordination between parenchyma and carbon storage

Carbon storage within sapwood buffers the imbalance between the supply and demand of carbon, contributing to the survival of trees in a changing environment, particularly under drought conditions (Chapin et al. 1990, McDowell et al. 2008,

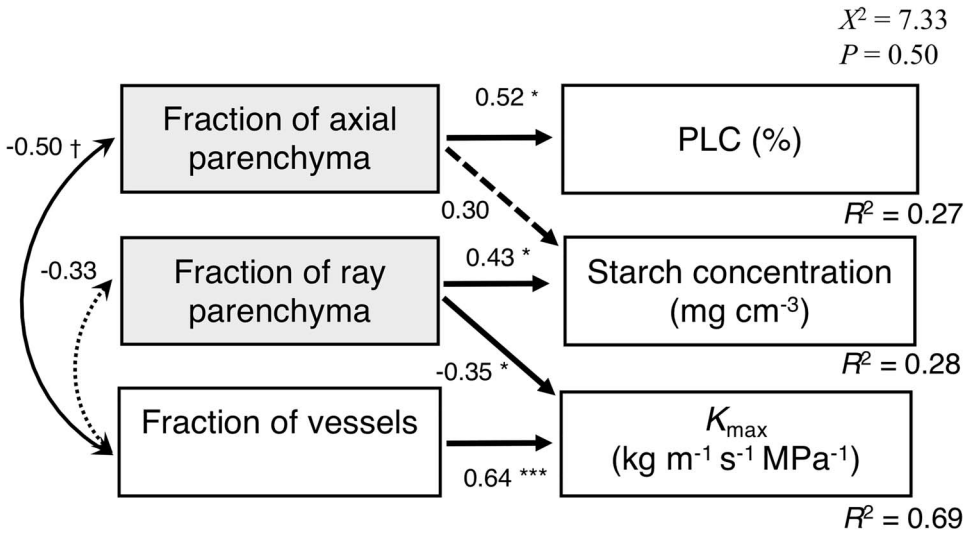

Figure 5. Path model for the relationships between xylem anatomy and functions among 15 woody species in the Bonin Islands, Japan. The overall model fit was evaluated by X^2-test and selected from alternative models by AIC comparisons. R^2 values represent the proportion of interspecific variance explained. Unidirectional arrows indicate direct paths from one variable to another one and bidirectional arrows indicate correlations between two variables. Numbers and symbols on arrows indicate standardized partial regression coefficients and significant levels, respectively. Dotted lines indicate non-significant paths. Parenchyma traits were filled with light gray. ***$P < 0.001$; *$P < 0.05$; †$0.05 \leq P < 0.10$.

Hartmann and Trumbore 2016, Yoshimura et al. 2016, Kono et al. 2019). Thus, clarifying the control of carbon storage within sapwood would provide an insight into the responses of trees to drought. In this study, we showed that fractions of RP and AP were positively associated with the storage of starch and NSC (Figures 2 and 5, Table 2). Although similar correlations have been observed in temperate forests with distinct dormant seasons (Plavcová et al. 2016, Chen et al. 2020, Pratt et al. 2021), our study was the first to investigate this using evergreen trees in a subtropical climate, emphasizing the importance of anatomical constraints for sapwood carbon stores. However, our NSC measurement was carried out only in summer, when a high level of starch is expected (our unpublished data)—probably associated with greater constraints on carbon demand than carbon uptake by drought (Würth et al. 2005). As such, the storage capacity of individual parenchyma cells may have reached their maxima. Thus, future studies should examine whether parenchyma fraction precisely predicts carbon storage in different species, regardless of its seasonal variations (Hoch et al. 2003, Würth et al. 2005, Martínez-Vilalta et al. 2016). In addition, anatomical properties other than parenchyma may additionally influence carbon storage (Plavcová et al. 2016, Pratt et al. 2021). For example, *L. micranthum* was found to have a high NSC content for low fractions of parenchyma because this species may store starch additionally in living fibers, which we did not consider.

In contrast to starch, the concentration of soluble sugars did not depend on parenchyma fraction across species. In this study, sampling was conducted in the summer, during which trees may allocate soluble sugars for various functions, such as respiration, osmoregulation and the recovery of hydraulic conductivity (Salleo et al. 2004, Hartmann and Trumbore 2016, Kono et al. 2019) in a species-specific manner (Yoshimura et al. 2016). If so, the content of soluble sugars in each parenchyma cell would differ among species, and the total sugar content within xylem would not be related to the amount of parenchyma.

Coordination between parenchyma fraction with sapwood density

The spatial trade-off for vessels, fibers and parenchyma potentially results in a trade-off between xylem functions (Pratt and Jacobsen 2017). An increased parenchyma fraction decreased the vessel and fiber fractions, but did not lower sapwood density (Table 2), which was consistent with previous studies (Poorter et al. 2010, Zheng and Martínez-Cabrera 2013, Ziemińska et al. 2015, Janssen et al. 2020). This independence was the same for RP and AP, suggesting that parenchyma fraction does not influence sapwood density, and thus the mechanical strength (stiffness and fracture toughness) of the xylem for the species studied. Because wood density is often strongly and negatively correlated with hydraulic capacitance (Meinzer et al. 2003, 2008, Scholz et al. 2007), parenchyma fraction would not be related to capacitance, as found in previous studies (Jupa et al. 2016, Ziemińska et al. 2020). Alternatively, our results suggest that hydraulic capacitance is more highly associated with vessel anatomy, such as vessel fraction and potential conductivity (Figure 3b and Table 2) or vessel contact fractions with fibers or parenchyma (Ziemińska et al. 2020), consistent with the observation that the main water source of capacitance during the early dehydration phase is from vessels (Yazaki et al. 2020).

Combining such a high capacitance with conductive vessels may prevent the drop in XWP during mild drought conditions (Table 2).

Overall coordination between xylem anatomy and function

Two covariation axes among the xylem functions existed across species, and AP and RP were involved in different axes (Figure 4). In the first axis, which accounted for 33.2% of the total variation, negative relationships were observed between the maximum water conductivity (K_{max} and K_p) and concentrations of soluble sugars and starch, wood density and resistance to vessel implosion (RI), suggesting that xylem hydraulic efficiency trades off with storage function, mechanical strength and possibly cavitation resistance. These relationships partially reflect the negative relationship between the fraction of vessels and that of the total and RP; that is, the increased vessel fraction enhances conductivity, but lowers the carbon storage capacity by decreasing parenchyma fraction. The second axis, which accounted for 31.2% of the total variation, represented the relationships between the native cavitation level and AP and vessel anatomy, such that xylem with a high fraction of AP and APV, and large vessels is associated with greater cavitation level. Some relationships in the above trade-offs have been demonstrated in previous studies (Hacke et al. 2001, Santiago et al. 2004, Jacobsen et al. 2005, Preston et al. 2006, Pratt and Jacobsen 2017, but for hydraulic efficiency *vs*. cavitation resistance, see Gleason et al. 2016*a*, Sanchez-Martinez et al. 2020). However, in this study, we proposed that, in addition to vessel anatomy, the carbon storage and parenchyma fraction are also important factors related to covariations in xylem function.

Conclusion

This study evaluated the coordination between parenchyma fraction and xylem hydraulic properties and storage capacity of NSC using 15 drought-adapted woody species on a subtropical island. The fraction of AP, especially that of APV, was positively correlated with the native cavitation level during the summer. The fraction of RP was negatively correlated with xylem hydraulic efficiency, and higher fractions of RP and AP were associated with high starch storage capacity. These results suggest that parenchyma fraction underlies species variation in xylem hydraulic and carbon use strategies, wherein xylem with a high fraction of AP and APV may adopt an embolism repair strategy through an increased storage of starch with low cavitation resistance. We suggest that investigations of parenchyma anatomy and its associations with other tissues would provide further insights into the resource use strategies of water and carbon, and therefore the life history strategies, of woody plants.

Supplementary data

Supplementary data for this article is available at *Tree Physiology* online.

Acknowledgments

Dr Y. Sano helped with cell identification. Drs N. Okada and H. Tobita supported the microscopic measurements. Drs K. Yoshimura, Y. Sano, T. Nakano, T. Sakata, Mrs S. Matsuyama, T. Suzuki and Y. Oka helped the sampling in the field. Dr Jordi Martínez-Vilalta and three anonymous reviewers made valuable suggestions for improving the manuscript. The Forest Agency of Japan and the local government of Tokyo Metropolitan permitted us to conduct this research.

Conflicts of interest

None declared.

Funding

This study was funded by grants-in-aid from the Japan Society for the Promotion of Science (nos. 18H04149 to A.I. and 20J01359 to K.K.)

Author's contributions

KK and AI designed the study. KK, KM, TN and AI completed the measurements. KK analyzed the data. KK wrote the paper with contributions from STS, KY and AI.

References

Ackerly DD (2000) Taxon sampling, correlated evolution, and independent contrasts. Evolution 54:1480–1492.

Alvarez-Clare S, Kitajima K (2007) Physical defence traits enhance seedling survival of neotropical tree species. Funct Ecol 21:1044–1054.

Aritsara ANA, Razakandraibe VM, Ramananantoandro T, Gleason SM, Cao K (2021) Increasing axial parenchyma fraction in the Malagasy Magnoliids facilitated the co-optimisation of hydraulic efficiency and safety. New Phytol 229:1467–1480.

Brodersen CR, McElrone AJ (2013) Maintenance of xylem network transport capacity: a review of embolism repair in vascular plants. Front Plant Sci 4:1–11.

Carlquist S (2018) Living cells in wood 3. Overview; functional anatomy of the parenchyma network. Bot Rev 84:242–294.

Chapin FS, Schulze E, Mooney HA (1990) The ecology and economics of storage in plants. Annu Rev Ecol Syst 21:423–447.

Chave J, Coomes D, Jansen S, Lewis SL, Swenson NG, Zanne AE (2009) Towards a worldwide wood economics spectrum. Ecol Lett 12:351–366.

Chen Z, Zhu S, Zhang Y, Luan J, Li S, Sun P, Wan X, Liu S (2020) Trade-off between storage capacity and embolism resistance in the xylem of temperate broadleaf tree species. Tree Physiol 40:1029–1042.

Choat B, Cobb AR, Jansen S (2008) Structure and function of bordered pits: new discoveries and impacts on whole-plant hydraulic function. New Phytol 177:608–626.

Davis SD, Sperry JS, Hacke UG (1999) The relationship between xylem conduit diameter and cavitation caused by freezing. Am J Bot 86:1367–1372.

Dória LC, Podadera DS, del Arco M, Chauvin T, Smets E, Delzon S, Lens F (2018) Insular woody daisies (*Argyranthemum*, Asteraceae) are more resistant to drought-induced hydraulic failure than their herbaceous relatives. Funct Ecol 32:1467–1478.

Dubois M, Gilles K, Hamilton JK, Rebers PA, Smith F (1951) A colorimetric method for the determination of sugars. Nature 168:167.

Felsenstein J (1985) Phylogenies and the comparative method. Am Nat 125:1–15.

Fichtler E, Worbes M (2012) Wood anatomical variables in tropical trees and their relation to site conditions and individual tree morphology. IAWA J 33:119–140.

Fortunel C, Ruelle J, Beauchêne J, Fine PVA, Baraloto C (2014) Wood specific gravity and anatomy of branches and roots in 113 Amazonian rainforest tree species across environmental gradients. New Phytol 202:79–94.

Fromard L, Babin V, Fleurat-Lessard P, Fromont JC, Serrano R, Bonnemain JL (1995) Control of vascular sap pH by the vessel-associated cells in woody species: physiological and immunological studies. Plant Physiol 108:913–918.

van Gelder HA, Poorter L, Sterck FJ (2006) Wood mechanics, allometry, and life-history variation in a tropical rain forest tree community. New Phytol 171:367–378.

Gleason SM, Westoby M, Jansen S et al. (2016*a*) Weak tradeoff between xylem safety and xylem-specific hydraulic efficiency across the world's woody plant species. New Phytol 209:123–136.

Gleason SM, Westoby M, Jansen S et al. (2016*b*) On research priorities to advance understanding of the safety–efficiency tradeoff in xylem. New Phytol 211:1156–1158.

Hacke UG, Sperry JS (2001) Functional and ecological xylem anatomy. Perspect Plant Ecol Evol Syst 4:97–115.

Hacke UG, Sperry JS, Pockman WT, Davis SD, McCulloh KA (2001) Trends in wood density and structure are linked to prevention of xylem implosion by negative pressure. Oecologia 126:457–461.

Hacke UG, Spicer R, Schreiber SG, Plavcová L (2017) An ecophysiological and developmental perspective on variation in vessel diameter. Plant Cell Environ 40:831–845.

Hartmann H, Trumbore S (2016) Understanding the roles of nonstructural carbohydrates in forest trees – from what we can measure to what we want to know. New Phytol 211:386–403.

Hoch G, Richter A, Korner C (2003) Non-structural carbon compounds in temperate forest trees. Plant Cell Environ 26:1067–1081.

Ishida A, Nakano T, Yazaki K, Matsuki S, Koike N, Lauenstein DL, Shimizu M, Yamashita N (2008) Coordination between leaf and stem traits related to leaf carbon gain and hydraulics across 32 drought-tolerant angiosperms. Oecologia 156:193–202.

Jacobsen AL, Agenbag L, Esler KJ, Pratt RB, Ewers FW, Davis SD (2007) Xylem density, biomechanics and anatomical traits correlate with water stress in 17 evergreen shrub species of the Mediterranean-type climate region of South Africa. J Ecol 95:171–183.

Jacobsen AL, Brandon Pratt R, Tobin MF, Hacke UG, Ewers FW (2012) A global analysis of xylem vessel length in woody plants. Am J Bot 99:1583–1591.

Jacobsen AL, Ewers FW, Pratt RB, Paddock WA III, Davis SD (2005) Do xylem fibers affect vessel cavitation resistance? Plant Physiol 139:546–556.

Janssen TAJ, Hölttä T, Fleischer K, Naudts K, Dolman H (2020) Wood allocation trade-offs between fiber wall, fiber lumen, and axial parenchyma drive drought resistance in neotropical trees. Plant Cell Environ 43:965–980.

Jupa R, Plavcová L, Gloser V, Jansen S (2016) Linking xylem water storage with anatomical parameters in five temperate tree species. Tree Physiol 36:756–769.

Kiorapostolou N, Da Sois L, Petruzzellis F, Savi T, Trifilò P, Nardini A, Petit G (2019) Vulnerability to xylem embolism correlates to wood parenchyma fraction in angiosperms but not in gymnosperms. Tree Physiol 39:1675–1684.

Knipfer T, Cuneo IF, Brodersen CR, McElrone AJ (2016) In situ visualization of the dynamics in xylem embolism formation and removal in the absence of root pressure: a study on excised grapevine stems. Plant Physiol 171:1024–1036.

Kono Y, Ishida A, Saiki S-T, Yoshimura K, Dannoura M, Yazaki K, Kimura F, Yoshimura J, Aikawa S (2019) Initial hydraulic failure followed by late-stage carbon starvation leads to drought-induced death in the tree *Trema orientalis*. Commun Biol 2:8.

Liu W, Su J, Li S, Lang X, Huang X (2018) Non-structural carbohydrates regulated by season and species in the subtropical monsoon broad-leaved evergreen forest of Yunnan Province, China. Sci Rep 8:1–10.

Loepfe L, Martinez-Vilalta J, Piñol J, Mencuccini M (2007) The relevance of xylem network structure for plant hydraulic efficiency and safety. J Theor Biol 247:788–803.

Martínez-Cabrera HI, Jones CS, Espino S, Jochen Schenk H (2009) Wood anatomy and wood density in shrubs: responses to varying aridity along transcontinental transects. Am J Bot 96:1388–1398.

Martínez-Vilalta J, Sala A, Asensio D, Galiano L, Hoch G, Palacio S, Piper FI, Lloret F (2016) Dynamics of non-structural carbohydrates in terrestrial plants: a global synthesis. Ecol Monogr 86: 495–516.

McDowell N, Pockman WT, Allen CD et al. (2008) Mechanisms of plant survival and mortality during drought: why do some plants survive while others succumb to drought? New Phytol 178:719–739.

Meinzer FC, Campanello PI, Domec JC, Gatti MG, Goldstein G, Villalobos-Vega R, Woodruff DR (2008) Constraints on physiological function associated with branch architecture and wood density in tropical forest trees. Tree Physiol 28:1609–1617.

Meinzer FC, James SA, Goldstein G, Woodruff D (2003) Whole-tree water transport scales with sapwood capacitance in tropical forest canopy trees. Plant Cell Environ 26:1147–1155.

Méndez-Alonzo R, Paz H, Cruz R, Rosell JA, Olson ME (2012) Coordinated evolution of leaf and stem economics in tropical dry forest trees. Ecology 93:2397–2406.

Morris H, Brodersen C, Schwarze FWMR, Jansen S (2016*a*) The parenchyma of secondary xylem and its critical role in tree defense against fungal decay in relation to the CODIT model. Front Plant Sci 7:1–18.

Morris H, Gillingham MAF, Plavcová L et al. (2018*a*) Vessel diameter is related to amount and spatial arrangement of axial parenchyma in woody angiosperms. Plant Cell Environ 41:245–260.

Morris H, Hietala AM, Jansen S, Ribera J, Rosner S, Salmeia KA, Schwarze FWMR (2020) Using the CODIT model to explain secondary metabolites of xylem in defence systems of temperate trees against decay fungi. Ann Bot 125:701–720.

Morris H, Jansen S (2016) Secondary xylem parenchyma - from classical terminology to functional traits. IAWA J 37:1–15.

Morris H, Plavcová L, Cvecko P et al. (2016*b*) A global analysis of parenchyma tissue fractions in secondary xylem of seed plants. New Phytol 209:1553–1565.

Morris H, Plavcová L, Gorai M, Klepsch MM, Kotowska M, Jochen Schenk H, Jansen S (2018*b*) Vessel-associated cells in angiosperm xylem: highly specialized living cells at the symplast-apoplast boundary. Am J Bot 105:151–160.

Paradis E, Claude J, Strimmer K (2004) APE: analyses of phylogenetics and evolution in R language. Bioinformatics 20:289–290.
Plavcová L, Gallenmüller F, Morris H, Khatamirad M, Jansen S, Speck T (2019) Mechanical properties and structure-function trade-offs in secondary xylem of young roots and stems. J Exp Bot 70:3679–3691.
Plavcová L, Hoch G, Morris H, Ghiasi S, Jansen S (2016) The amount of parenchyma and living fibers affects storage of nonstructural carbohydrates in young stems and roots of temperate trees. Am J Bot 103:603–612.
Poorter L, McDonald I, Alarcón A, Fichtler E, Licona J-C, Peña-Claros M, Sterck F, Villegas Z, Sass-Klaassen U (2010) The importance of wood traits and hydraulic conductance for the performance and life history strategies of 42 rainforest tree species. New Phytol 185:481–492.
Pratt RB, Jacobsen AL (2017) Conflicting demands on angiosperm xylem: tradeoffs among storage, transport and biomechanics. Plant Cell Environ 40:897–913.
Pratt RB, Jacobsen AL, Ewers FW, Davis SD (2007) Relationships among xylem transport, biomechanics and storage in stems and roots of nine Rhamnaceae species of the California chaparral. New Phytol 174:787–798.
Pratt RB, Tobin MF, Jacobsen AL et al. (2021) Starch storage capacity of sapwood is related to dehydration avoidance during drought. Am J Bot 108:91–101.
Preston KA, Cornwell WK, Denoyer JL (2006) Wood density and vessel traits as distinct correlates of ecological strategy in 51 California coast range angiosperms. New Phytol 170:807–818.
Core Team R (2019) R: A language and environment for statistical computing. R Foundation for Statistical Computing.
Rosseel Y (2012) Lavaan: an R package for structural equation modeling and more version 0.5-12 (BETA). J Stat Softw 48:1–36.
Saiki ST, Ishida A, Yoshimura K, Yazaki K (2017) Physiological mechanisms of drought-induced tree die-off in relation to carbon, hydraulic and respiratory stress in a drought-tolerant woody plant. Sci Rep 7:1–7.
Salleo S, Lo Gullo MA, Trifilò P, Nardini A (2004) New evidence for a role of vessel-associated cells and phloem in the rapid xylem refilling of cavitated stems of *Laurus nobilis* L. Plant Cell Environ 27:1065–1076.
Sanchez-Martinez P, Martínez-Vilalta J, Dexter KG, Segovia RA, Mencuccini M (2020) Adaptation and coordinated evolution of plant hydraulic traits. Ecol Lett 23:1599–1610.
Santiago LS, Goldstein G, Meinzer FC, Fisher JB, Machado K, Woodruff D, Jones T (2004) Leaf photosynthetic traits scale with hydraulic conductivity and wood density in Panamanian forest canopy trees. Oecologia 140:543–550.
Schenk HJ, Espino S, Romo DM et al. (2017) Xylem surfactants introduce a new element to the cohesion-tension theory. Plant Physiol 173:1177–1196.
Schindelin J, Arganda-Carreras I, Frise E et al. (2012) Fiji: an open-source platform for biological-image analysis. Nat Methods 9:676–682.
Scholz FG, Bucci SJ, Goldstein G, Meinzer FC, Franco AC, Miralles-Wilhelm F (2007) Biophysical properties and functional significance of stem water storage tissues in Neotropical savanna trees. Plant Cell Environ 30:236–248.
Schulte PJ, Gibson AC, Nobel PS (1987) Xylem anatomy and hydraulic conductance of *Psilotum nudum*. Am J Bot 74:1438.
Scoffoni C, Sack L (2017) The causes and consequences of leaf hydraulic decline with dehydration. J Exp Bot 68:4479–4496.
Secchi F, Pagliarani C, Zwieniecki MA (2017) The functional role of xylem parenchyma cells and aquaporins during recovery from severe water stress. Plant Cell Environ 40:858–871.
Secchi F, Zwieniecki MA (2012) Analysis of xylem sap from functional (nonembolized) and nonfunctional (embolized) vessels of *Populus nigra*: chemistry of refilling. Plant Physiol 160:955–964.
Shimizu Y (1992) Origin of *Distylium* dry forest and occurrence of endangered species in the Bonin Islands. Pacific Sci 46: 179–196.
Slik JWF, Franklin J, Arroyo- V et al. (2018) Phylogenetic classification of the world's tropical forests. Proc Natl Acad Sci 115:E3067.
Sperry JS, Donnelly JR, Tyree MT (1988) A method for measuring hydraulic conductivity and embolism in xylem. Plant Cell Environ 11:35–40.
Sperry JS, Hacke UG, Pittermann J (2006) Size and function in conifer tracheids and angiosperm vessels. Am J Bot 93:1490–1500.
Spicer R (2014) Symplasmic networks in secondary vascular tissues: parenchyma distribution and activity supporting long-distance transport. J Exp Bot 65:1829–1848.
Spicer R, Holbrook NM (2007) Parenchyma cell respiration and survival in secondary xylem: does metabolic activity decline with cell age? Plant Cell Environ 30:934–943.
Torres-Ruiz JM, Jansen S, Choat B et al. (2015) Direct X-ray microtomography observation confirms the induction of embolism upon xylem cutting under tension. Plant Physiol 167:40–43.
Trifilò P, Raimondo F, Lo Gullo MA, Barbera PM, Salleo S, Nardini A (2014) Relax and refill: xylem rehydration prior to hydraulic measurements favours embolism repair in stems and generates artificially low PLC values. Plant Cell Environ 37:2491–2499.
Tyree MT, Zimmermann MH (2002) Xylem structure and the ascent of sap, 2nd edn. Springer-Verlag, Berlin.
Venturas MD, Mackinnon ED, Jacobsen AL, Pratt RB (2015) Excising stem samples underwater at native tension does not induce xylem cavitation. Plant Cell Environ 38:1060–1068.
Warton DI, Duursma RA, Falster DS, Taskinen S (2012) smatr 3- an R package for estimation and inference about allometric lines. Methods Ecol Evol 3:257–259.
Warton DI, Hui FKC (2011) The arcsine is asinine: the analysis of proportions in ecology. Ecology 92:3–10.
Webb CO, Donoghue MJ (2005) Phylomatic: tree assembly for applied phylogenetics. Mol Ecol Notes 5:181–183.
Wheeler JK, Huggett BA, Tofte AN, Rockwell FE, Holbrook NM (2013) Cutting xylem under tension or supersaturated with gas can generate PLC and the appearance of rapid recovery from embolism. Plant Cell Environ 36:1938–1949.
Wheeler JK, Sperry JS, Hacke UG, Hoang N (2005) Inter-vessel pitting and cavitation in woody Rosaceae and other vessel led plants: a basis for a safety versus efficiency trade-off in xylem transport. Plant Cell Environ 28:800–812.
Würth MKR, Peláez-Riedl S, Wright SJ, Körner C (2005) Non-structural carbohydrate pools in a tropical forest. Oecologia 143:11–24.
Yazaki K, Levia DF, Takenouchi A et al. (2020) Imperforate tracheary elements and vessels alleviate xylem tension under severe dehydration: insights from water release curves for excised twigs of three tree species. Am J Bot 107:1122–1135.
Yonekura K, Kajita T (2003) BGPlants: Japanese scientific name index (YList).
Yoshida K, Iijima Y (2009) Hydroclimatic conditions during the last decade in the Ogasawara (Bonin) Islands. Japanese J Limnol 70:13–20.
Yoshimura K, Saiki ST, Yazaki K, Ogasa MY, Shirai M, Nakano T, Yoshimura J, Ishida A (2016) The dynamics of carbon stored in xylem sapwood to drought-induced hydraulic stress in mature trees. Sci Rep 6:24513.
Zanne AE, Tank DC, Cornwell WK et al. (2014) Three keys to the radiation of angiosperms into freezing environments. Nature 506:89–92.

Zheng J, Martínez-Cabrera HI (2013) Wood anatomical correlates with theoretical conductivity and wood density across China: evolutionary evidence of the functional differentiation of axial and radial parenchyma. Ann Bot 112:927–935.

Zheng J, Zhao X, Morris H, Jansen S (2019) Phylogeny best explains latitudinal patterns of xylem tissue fractions for woody angiosperm species across China. Front Plant Sci 10:1–12.

Ziemińska K, Butler DW, Gleason SM, Wright IJ, Westoby M (2013) Fibre wall and lumen fractions drive wood density variation across 24 Australian angiosperms. AoB Plants 5: 1–14.

Ziemińska K, Rosa E, Gleason SM, Holbrook NM (2020) Wood day capacitance is related to water content, wood density, and anatomy across 30 temperate tree species. Plant Cell Environ 43: 3048–3067.

Ziemińska K, Westoby M, Wright IJ (2015) Broad anatomical variation within a narrow wood density range - a study of twig wood across 69 Australian angiosperms. PLoS One 10:e0124892.